

State-space representation of radiation forces in time-domain vessel models¶

ERLEND KRISTIANSSEN†*, ÅSMUND HJULSTAD‡ and
OLAV EGELAND†

Keywords: State-space realization, Frequency-dependent characteristics, Time-domain, Convolution integral, Discretization

The paper presents a method for generating a new and efficient time-domain formulation of the equations of motion for a vessel with frequency-dependent hydrodynamic coefficients. Previous work on this topic has relied on the use of convolution terms, whereas in this work state-space models are used. This leads to a model formulation that is well suited for controller design and simulation.

1. Introduction

The concept of frequency-dependent added mass and potential damping is well established in the formulation of the equations of motion for a surface vessel (Ogilvie, 1964). This formulation is used in identification experiments for ship models using motion at a single frequency, and it is used in commercially available programs like WAMIT and VERES. It was shown in Cummins (1962), that the frequency dependence of added mass and potential damping can be seen as a consequence of a convolution term in the radiation potential. The convolution term in the radiation potential leads to a convolution term in the equation of motion (Cummins, 1962; Ogilvie, 1964). For motion at a single frequency, the convolution term in the equation of motion can be represented by frequency-dependent added mass and potential damping parameters. The formulations of the equation of motion based on the use of convolution terms, or alternatively, on frequency-dependent parameters are not in agreement with the model formulations used in simulation and in automatic control. As a result of this it is not straightforward to apply the usual methods for simulation and for controller analysis and design. This provides the motivation for investigating this problem further.

The main contribution of the present paper is to show how the equations of motion for a surface vessel can be reformulated into a state-space form suited for simulation and controller design. Moreover, it is shown that analysis based on the Laplace transformation, state-space models and energy considerations provides additional insight into the radiation problem. We propose a new method that generates a low order state-space model from frequency-dependent added mass and frequency-dependent potential damping as obtained from identification experiments or numerical computations. The resulting

*Corresponding author. E-mail addresses: erlend.kristiansen@ntnu.no (E. Kristiansen), olav.egeland@ntnu.no (O. Egeland).

†Centre for Ships and Ocean Structures, NO-7491 Trondheim Norway.

‡Norwegian University of Science and Technology, NO-7491 Trondheim, Norway.

¶Reprinted from *Ocean Engineering*, 32, Erlend Kristiansen, Åsmund Hjulstad, Olav Egeland, State-space representation of radiation forces in time-domain vessel models, 2195–2216, Copyright (2005), with permission from Elsevier.

model gives an accurate and computationally efficient representation of the convolution term. This method is applied to detailed data from the panel method program WAMIT for an offshore support vessel. It is shown that an accurate representation of all first-order wave effects was achieved with eight states for each convolution term in the complete equations of motion. The resulting state-space model is implemented in Simulink in the Matlab program package, and simulations are performed.

Related work has been done for an oscillating water column in Yu and Falnes (1995) and Yu and Falnes (1998). However, for the vessel models of this study, the approach used in these works was found to be computationally ineffective, and impractical to combine with already established methods for system identification and model reduction.

2. Preliminaries

2.1. Introduction

In this section we will present background material needed for the presentation of the main results in Section 3.

The usual method for finding the hydrodynamic forces acting on a ship moving in waves, is based on the superposition of the radiation forces due to the ship motion in an undisturbed sea, and of the diffraction forces due to the wave forces on a non-moving ship (Newman, 1977). Irrotational flow of an inviscid and incompressible fluid is assumed. The velocity potential ϕ is then described as the sum $\phi = \phi_R + \phi_D$, where the radiation potential ϕ_R is due to the motion of the ship on an undisturbed sea, and the diffraction potential ϕ_D is due to the wave excitation. The pressure on the hull is assumed to be given by

$$p = -\rho gz - \rho \frac{\partial \phi_R}{\partial t} - \rho \frac{\partial \phi_D}{\partial t} \quad (1)$$

which is a sum of hydrostatic pressure, radiation pressure and diffraction pressure. The inertial coordinate system is shown in Figure 1, with x pointing in the bow direction of the ship, z pointing in the upward vertical direction, and y given by the right-hand rule. Note that $z = 0$ is placed on the undisturbed free surface. The force \vec{F} and the moment

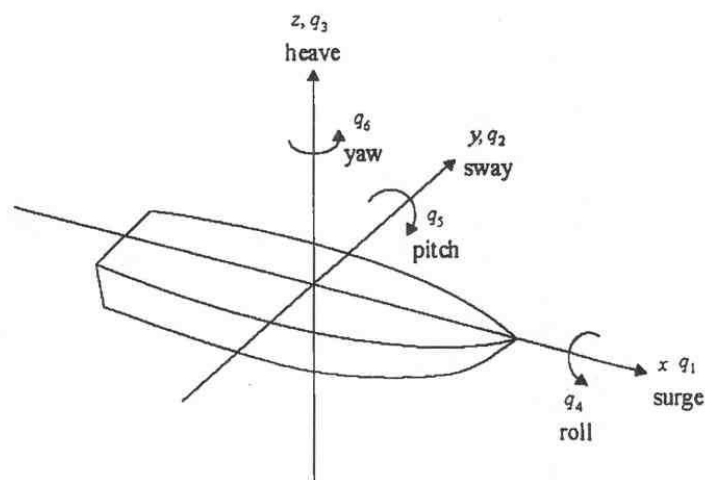


Figure 1. Coordinate system with generalized coordinates.

\vec{M} on the ship hull can then be described as sums of hydrostatic terms, radiation effects and diffraction effects. The radiation force and the radiation moment are given by

$$\vec{F}^R = -\rho \iint_{S_B} \vec{n} \frac{\partial \phi_R}{\partial t} dA \quad (2)$$

$$\vec{M}^R = -\rho \iint_{S_B} (\vec{r} \times \vec{n}) \frac{\partial \phi_R}{\partial t} dA \quad (3)$$

For notational simplicity the motion is described with generalized coordinates $q = (q_1 \dots q_6)^T$ as shown in Figure 1, and associated generalized forces $\tau = (\tau_1 \dots \tau_6)^T$. The results can be extended to the usual kinematics as given in Fossen (1994). The equation of motion is given by

$$\sum_{k=1}^6 m_{jk} \ddot{q}_k = \tau_j^H + \tau_j^R + \tau_j^D + \tau_j^A + \tau_j^E \quad (4)$$

where m_{jk} are the inertia parameters of the ship, τ_j^H are the hydrostatic forces, τ_j^R are the radiation forces, τ_j^D are the diffraction forces, τ_j^A are the actuator forces, and τ_j^E are the external forces.

2.2. The radiation problem with memory effects

To simplify the presentation, we will consider a ship with no forward speed. It is straightforward to extend these results to a ship with a steady forward speed as in Ogilvie (1964).

Define \vec{r} as the position vector of a point on the hull surface S , measured in a fixed reference system, and \vec{r}_B as the position vector of the same point, but measured in a reference system moving with the hull. When the ship is in its equilibrium position, the two position vectors are assumed to coincide. The deflection of any point of the hull can now be written as

$$\vec{r} - \vec{r}_B = \sum_{i=1}^6 \vec{q}_i(\vec{r}, t) \quad (5)$$

where

$$\vec{q}_i(\vec{r}, t) = \begin{cases} q_i(t) \vec{i}_i, & i = 1-3 \\ q_i(t) \vec{i}_{i-3} \times \vec{r}, & i = 4-6 \end{cases} \quad (6)$$

are the deflections in surge, sway or heave for $i = 1-3$, respectively, and the rotations in roll, pitch and yaw for $i = 4-6$, respectively. It is assumed that the deviations $q_i(t)$ are sufficiently small so that second-order errors can be left out of the analysis. Thus, \vec{r}_B can be used as argument for \vec{q}_i , as only second-order errors occur from this. The radiation potential ϕ_R must satisfy certain general boundary conditions (Ogilvie, 1964), that are omitted here for the sake of brevity.

A solution that satisfies the general boundary conditions is (Cummins, 1962)

$$\phi_R(\vec{r}, t) = \sum_{i=1}^6 \dot{q}_i(t) \psi_i(\vec{r}) + \sum_{i=1}^6 \int_{-\infty}^t \chi_i(\vec{r}, t-\tau) \dot{q}_i(\tau) d\tau \quad (7)$$

where ψ_i and $\chi_i(\vec{r}, t)$ satisfies certain specific boundary conditions (Ogilvie, 1964).

The physical interpretation of the potentials $\psi_i(\vec{r})$ and $\chi_i(\vec{r}, t)$ is made clear by considering an impulse in the velocity $\dot{q}_{i=k}$, which is equivalent to a step in $q_{i=k}$. The resulting radiation potential is

$$\dot{q}_k = \delta(t) \Rightarrow \phi_R(\vec{r}, t) = \delta(t)\psi_k(\vec{r}) + \chi_k(\vec{r}, t) \quad (8)$$

It is seen that the potentials $\psi_i(\vec{r})$ represent the instantaneous response of the fluid due to the ship motion, whereas $\chi_i(\vec{r}, t)$ are impulse responses to the ship velocity.

2.3. Equation of motion including memory effects

The radiation force can be written

$$\begin{aligned} \tau_j^R = & \tau_{sj}^R - \sum_{k=1}^6 b_{jk} \ddot{q}_k - \sum_{k=1}^6 b_{jk} \dot{q}_k - \sum_{k=1}^6 c_{jk} q_k \\ & - \sum_{k=1}^6 \int_{-\infty}^t K_{jk}(t-\sigma) \dot{q}_k(\sigma) d\sigma \end{aligned} \quad (9)$$

where $\tau_{s,j}^R$ represent a steady radiation force due to a steady forward speed. It is noted that in Newman (1977), the radiation potential is assumed to be $\phi_R = \sum_{i=1}^6 \dot{q}_i \psi_i$, which means that the convolution terms has been set to zero. Suppose that the velocity is a unit impulse $\dot{q}_k(t) = \delta(t)$. Then the convolution terms are given by

$$\int_{-\infty}^t K_{jk}(t-\sigma) \delta(\sigma) d\sigma = K_{jk}(t) \quad (11)$$

This means that $K_{jk}(t)$ is the impulse response function in direction j to an impulse in velocity in direction k . Note that if the positions were considered as the inputs, then $K_{jk}(t)$ would be step response functions.

The equation of motion is found to be

$$\sum_{k=1}^6 (m_{jk} + a_{jk}) \ddot{q}_k + \sum_{k=1}^6 b_{jk} \dot{q}_k + \sum_{k=1}^6 c_{jk} q_k + \sum_{k=1}^6 \int_{-\infty}^t K_{jk}(t-\sigma) \dot{q}_k(\sigma) d\sigma = \tau_{sj}^R + \tau_j^D + \tau_j^E \quad (12)$$

It is noted that the effect of wave excitation is captured by the diffraction force τ_j^D , and that wave excitation is not involved in the derivation of the convolution term of the radiation force. Moreover, it is noted that the derivation of (12) was done without resorting to frequency analysis results. In particular, the concept of frequency-dependent added mass and potential damping has not been introduced so far.

Equation (12) is a general equation of motion for a ship with a steady forward speed U . The calculation of the hydrodynamic coefficients a_{jk} , b_{jk} , c_{jk} can be done in several ways, but special consideration must be taken about the presence of a steady forward speed, as can be seen in previous equations. The program package WAMIT used in later simulations to calculate the hydrodynamic coefficients and frequency-dependent added mass and damping does not support the presence of a steady forward speed. Thus, following calculations are done assuming no forward speed. The only consequence of this in the form of (12), is that the steady radiation forces $\tau_{s,j}^R$ is set equal to zero. Moreover, for a vessel in steady forward translation, the steady radiation force $\tau_{s,j}^R$ will be cancelled by the actuator force τ_j^A .

2.4. Convolution terms from experimental data

The parameters of the equations of motion can be found from model experiments with single frequency motion $q_k(t) = q_k \cos \omega t$ with $q_k(t) = 0$ for $t < 0$. Then, according to standard arguments all terms in the equation of motion will eventually be sinusoidal and of the same frequency ω . In particular, we note that the convolution integral can be written (Ogilvie, 1964)

$$\begin{aligned} & \int_{-\infty}^t K_{jk}(t-\sigma) \dot{q}_k(\sigma) d\sigma \\ &= -\dot{q}_k(t) \left(\frac{1}{\omega} \int_0^{\infty} K_{jk}(\sigma) \sin \omega \sigma d\sigma \right) + \dot{q}_k(t) \left(\int_0^{\infty} K_{jk}(\sigma) \cos \omega \sigma d\sigma \right) \end{aligned} \quad (13)$$

This leads to the equation of motion in the widely used form

$$\sum_{k=1}^6 (m_{jk} + \alpha_{jk}(\omega)) \ddot{q}_k + \sum_{k=1}^6 \beta_{jk}(\omega) \dot{q}_k + \sum_{k=1}^6 c_{jk} q_k = \tau_j^D + \tau_j^A + \tau_j^E \quad (14)$$

where the frequency-dependent added mass $\alpha_{jk}(\omega)$ and the frequency-dependent potential damping parameters $\beta_{jk}(\omega)$ are given by

$$\alpha_{jk}(\omega) = a_{jk} - \frac{1}{\omega} \int_0^{\infty} K_{jk}(t) \sin \omega t dt \quad (15)$$

$$\beta_{jk}(\omega) = b_{jk} + \int_0^{\infty} K_{jk}(t) \cos \omega t dt \quad (16)$$

It is seen that this formulation captures the frequency dependence of the added mass and the potential damping parameters that is observed in identification experiments with single-frequency motion. However, the equation of motion in the form (14) is only valid under the assumptions that $q_k(t) = q_k \cos t$, and that τ_j^D and τ_j^A are sinusoidal functions at frequency ω . The model formulation (14) with frequency-dependent added mass and potential damping cannot be used to describe transient dynamics (Cummins, 1962). We therefore, turn our attention back to the formulation based on convolution terms, and develop this further.

The Fourier transformation $\hat{K}_{jk}(\omega)$ of the impulse response function $K_{jk}(t)$ is

$$\hat{K}_{jk}(\omega) = \int_0^{\infty} K_{jk}(t) \cos \omega t dt - j \int_0^{\infty} K_{jk}(t) \sin \omega t dt \quad (17)$$

where $j^2 = -1$. The impulse response $K_{jk}(t)$ may be assumed to be of finite energy (Ogilvie, 1964). Therefore, the Fourier transform $\hat{K}_{jk}(\omega)$ must converge to zero as the frequency ω tends to infinity, i.e. $\lim_{\omega \rightarrow \infty} \hat{K}_{jk}(\omega) = 0$. This implies that $\alpha_{jk}(\infty) = a_{jk}$ and $\beta_{jk}(\infty) = b_{jk}$, and it follows that $K_{jk}(t)$ can be found from either of the inverse $\alpha_{jk}(\infty) = a_{jk}$ transformations

$$K_{jk}(t) = -\frac{2}{\pi} \int_0^{\infty} \omega [\alpha_{jk}(\omega) - \alpha_{jk}(\infty)] \sin \omega t d\omega \quad (18)$$

$$K_{jk}(t) = -\frac{2}{\pi} \int_0^{\infty} [\beta_{jk}(\omega) - \beta_{jk}(\infty)] \cos \omega t d\omega \quad (19)$$

As (19) converges considerably faster than (18), (19) is used for computations.

2.5. Convolution

The concept of convolution in the time-domain is well established in linear systems theory for the description of linear time-invariant systems. Convolution integrals are closely related to Laplace transforms and state-space models, and as a background for the main result of the present paper a brief explanation of this is given.

Let $u(t)$ be a signal, and define the signal $y(t)$ by a convolution integral

$$y(t) = \int_{-\infty}^t H(t - \sigma)u(\sigma)d\sigma \quad (20)$$

where $H(t)$ is the kernel, which is assumed to be causal so that $H(t) = 0$, whenever $t < 0$. The Laplace transform $\mathcal{L}\{\cdot\}$ of the kernel $H(t)$ is the transfer function

$$\tilde{H}(s) = \mathcal{L}\{H(t)\} = \int_0^{\infty} H(t)e^{st} dt$$

Let the Laplace transforms of the signals $u(t)$ and $y(t)$ be denoted by

$$\tilde{u}(s) = \mathcal{L}\{u(t)\} = \int_0^{\infty} u(t)e^{st} dt \quad (21)$$

$$\tilde{y}(s) = \mathcal{L}\{y(t)\} = \int_0^{\infty} y(t)e^{st} dt \quad (22)$$

Then (20) implies that

$$\tilde{y}(s) = \tilde{H}(s)\tilde{u}(s) \quad (23)$$

Moreover, there exists a state-space realization of order n with a state vector $\mathbf{x}(t) \in \mathbb{R}^{n \times 1}$ and matrices $\mathbf{A} \in \mathbb{R}^{n \times n}$, $\mathbf{C} \in \mathbb{R}^{1 \times n}$ and $D \in \mathbb{R}$ so that

$$\dot{\mathbf{x}}(t) = \mathbf{A}\mathbf{x}(t) + \mathbf{B}u(t) \quad (24)$$

$$y(t) = \mathbf{C}\mathbf{x}(t) + Du(t) \quad (25)$$

The transfer function is given by the state-space realization according to

$$\tilde{H}(s) = \mathbf{C}(s\mathbf{I} - \mathbf{A})^{-1} + D \quad (26)$$

If the signal $u(t)$ is given, then the signal $y(t)$ can be calculated from a state-space realization using a time-integration method like a Runge-Kutta method. Calculation of $y(t)$ using a state-space realization is more efficient than a calculation based on the use of the convolution integral. Moreover, simulation packages like MATLAB and SIMULINK are based on the use of state-space formulations.

2.6. Model reduction

The main idea of this paper, which will be developed in the following sections, is to replace the computationally expensive convolution terms in the equations of motion with a state-space representation of low order. In the method we propose the convolution term is first converted to a high order state-space model. This high order state-space model is then converted to a low order state-space model that will approximate the convolution term with sufficient accuracy. This process of converting a high order state-space model to a low order approximate state-space model is called model reduction. In the work reported in this paper model reduction was performed using the

balanced truncation method. An overview on the balanced truncation method and other model reduction techniques can be found in the survey articles (Antoulas and Sorensen, 2001; Gugercin and Antoulas, 2000).

The balanced truncation method is described as follows. Consider a stable linear system of order n with scalar input u and scalar output y given by

$$\dot{\bar{\mathbf{x}}}(t) = \bar{\mathbf{A}}\bar{\mathbf{x}}(t) + \bar{\mathbf{B}}u(t) \quad (27)$$

$$y(t) = \bar{\mathbf{C}}\bar{\mathbf{x}}(t) + \bar{D}u(t) \quad (28)$$

where $\bar{\mathbf{A}} \in \mathbb{R}^{n \times n}$, $\bar{\mathbf{B}} \in \mathbb{R}^{n \times 1}$, $\bar{\mathbf{C}} \in \mathbb{R}^{1 \times n}$ and $\bar{D} \in \mathbb{R}$. The corresponding transfer function $\bar{H}(s)$ is given by

$$\bar{H}(s) = \bar{\mathbf{C}}(s\mathbf{I} - \bar{\mathbf{A}})^{-1} + \bar{D}. \quad (29)$$

Model reduction is used to approximate the system with a reduced system of order $k \ll n$ given by

$$\dot{\bar{\mathbf{x}}}(t) = \mathbf{A}\bar{\mathbf{x}}(t) + \mathbf{B}u(t) \quad (30)$$

$$y(t) = \mathbf{C}\bar{\mathbf{x}}(t) + Du(t) \quad (31)$$

where $\mathbf{A} \in \mathbb{R}^{k \times k}$, $\mathbf{B} \in \mathbb{R}^{k \times 1}$ and $\mathbf{C} \in \mathbb{R}^{1 \times k}$, and the associated approximate transfer function is

$$H(s) = \mathbf{C}(s\mathbf{I} - \mathbf{A})^{-1} + D \quad (31)$$

The accuracy of the approximation is characterized by the infinity norm $\|\cdot\|_\infty$ of the difference between the transfer functions $H(s)$ and $\bar{H}(s)$ defined by

$$\|\bar{H}(s) - H(s)\|_\infty = \sup_{\omega} |\bar{H}(j\omega) - H(j\omega)| \quad (33)$$

The balanced truncation algorithm can be written sequentially as:

- (1) Compute the Grammian matrices \mathcal{P} and \mathcal{Q} by solving the Lyapunov equations

$$\mathbf{A}\mathcal{P} + \mathcal{P}\mathbf{A}^T + \mathbf{B}\mathbf{B}^T = 0 \quad (34)$$

$$\mathbf{A}^T\mathcal{Q} + \mathcal{Q}\mathbf{A} + \mathbf{C}\mathbf{C}^T = 0 \quad (35)$$

- (2) Compute the controllability Cholesky factor \mathbf{L}_c and the observability Cholesky factor \mathbf{L}_o from $\mathcal{P} = \mathbf{L}_c^T\mathbf{L}_c$ and $\mathcal{Q} = \mathbf{L}_o^T\mathbf{L}_o$.
- (3) Compute the SVD

$$\mathbf{U}\Sigma\mathbf{V}^T = \mathbf{L}_o^T\mathbf{L}_c \quad (36)$$

where \mathbf{U} , \mathbf{V} have orthonormal columns and $\Sigma = \text{diag}(\sigma_1, \dots, \sigma_n)$, where $\sigma_1 \geq \sigma_2 \geq \dots \geq \sigma_n \geq 0$.

- (4) Compute the balancing transformation $\mathbf{T} = \mathbf{L}_c\mathbf{V}\Sigma^{-1/2}\mathbf{T}^{-1} = \Sigma^{-1/2}\mathbf{U}^T\mathbf{L}_o^T$.

- (5) Form the balanced realization as $\bar{\mathbf{A}}_b = \mathbf{T}^{-1}\bar{\mathbf{A}}\mathbf{T}$, $\bar{\mathbf{B}}_b = \mathbf{T}^{-1}\bar{\mathbf{B}}$, $\bar{\mathbf{C}}_b = \bar{\mathbf{C}}\mathbf{T}$.

- (6) Select the model order k and partition the matrices $\bar{\mathbf{A}}_b$, $\bar{\mathbf{B}}_b$, $\bar{\mathbf{C}}_b$ in the form

$$\bar{\mathbf{A}}_b = \begin{pmatrix} \mathbf{A} & \mathbf{A}_{12} \\ \mathbf{A}_{21} & \mathbf{A}_{22} \end{pmatrix}, \quad \bar{\mathbf{B}}_b = \begin{pmatrix} \mathbf{B} \\ \mathbf{B}_2 \end{pmatrix}, \quad \bar{\mathbf{C}}_b = (\mathbf{C} \quad \mathbf{C}_2) \quad (37)$$

where $\mathbf{A} \in \mathbb{R}^{k \times k}$, $\mathbf{B} \in \mathbb{R}^{k \times 1}$ and $\mathbf{C} \in \mathbb{R}^{1 \times k}$ in combination with D give the balanced truncation.

When model reduction with the balanced truncation technique is used, the reduced system will be stable, and the infinity norm of the approximation error will satisfy

$$\|\tilde{H}(s) - \bar{\tilde{H}}(s)\|_{\infty} \leq 2(\sigma_{k+1} + \dots + \sigma_n) \quad (38)$$

where σ_i are the diagonal entries of Σ as calculated in (36).

3. Proposed solution: state-space approximation of convolution terms

3.1. Outline

The formulations of the equation of motion based on the use of convolution terms are not in agreement with the model formulations used in simulation and in automatic control. As a result of this it is not straightforward to apply the usual methods for simulation and for controller analysis and design when convolution terms are present.

Given the radiation problem in the form

$$\sum_{k=1}^6 (m_{jk} + a_{jk})\ddot{q}_k + \sum_{k=1}^6 b_{jk}\dot{q}_k + \sum_{k=1}^6 c_{jk}q_k + \sum_{k=1}^6 \int_{-\infty}^t K_{jk}(t-\sigma)\dot{q}_k(\sigma)d\sigma = \tau_j^D + \tau_j^A + \tau_j^E \quad (39)$$

The following solution is proposed: the convolution term

$$\int_{-\infty}^t K_{jk}(t-\sigma)\dot{q}_k(\sigma)d\sigma$$

is replaced by μ_{jk} , which is the output of an approximate low order state-space model. This model is found by recognizing $K_{jk}(t)$ as the impulse response of the vessel motion $\dot{q}_k(t)$. The impulse response is used as input for a system identification method, yielding a high order state-space model, where the order depends on the temporal resolution of $K_{jk}(t)$. A model reduction method is then applied to yield a low order state-space model with output μ_{jk} .

3.2. The state-space representation

Convolution term j may be written

$$\mu_{jk} = \int_{-\infty}^t K_{jk}(t-\sigma)\dot{q}_k(\sigma)d\sigma \quad (40)$$

where we have introduced μ_{jk} as the output of a linear system with input \dot{q}_k and kernel $K_{jk}(t)$. Such a linear system can be represented by a state-space realization

$$\dot{\xi}_{jk} = \mathbf{A}_{jk}\xi_{jk} + \mathbf{B}_{jk}\dot{q}_k \quad (41)$$

$$\mu_{jk} = \mathbf{C}_{jk}\xi_{jk} + \mathbf{D}_{jk}\dot{q}_k \quad (42)$$

Given $K_{jk}(t)$, it is possible to find some state-space realization (41, 42) that given \dot{q}_k outputs μ_{jk} characterized according to (40). Then the equation of motion (39) can be written

$$\sum_{k=1}^6 (m_{jk} + a_{jk})\ddot{q}_k = - \sum_{k=1}^6 b_{jk}\dot{q}_k - \sum_{k=1}^6 c_{jk}q_k - \sum_{k=1}^6 \mu_{jk} + \tau_j^D + \tau_j^A + \tau_j^E \quad (43)$$

$$\dot{\xi}_{jk} = \mathbf{A}_{jk}\xi_{jk} + \mathbf{B}_{jk}\dot{q}_k \quad (44)$$

$$\mu_{jk} = \mathbf{C}_{jk}\xi_{jk} + \mathbf{D}_{jk}\dot{q}_k \quad (45)$$

As can be seen, the entire equation of motion is on state-space form. Having a complete state-space model will require far less computational power, not to mention processing memory, than a mixed model incorporating convolution terms. Thus, this model will be suited for implementation in digital controllers commonly used in control applications. In addition, a vast number of analysis and control design tools become available.

4. Analysis of state-space model using energy considerations

4.1. Passivity of the radiation problem

In this section the passivity properties of the radiation forces will be investigated (Egeland and Gravdahl, 2002). This can be done by assuming that $\phi_D = 0$, as superposition is assumed. The vessel motion given by the velocities \dot{q}_k induces fluid motion described by the radiation potential ϕ_R . The energy

$$V_R = \frac{1}{2} \sum_{k=1}^6 \sum_{j=1}^6 [a_{jk} \dot{q}_k \dot{q}_j + c_{jk} q_k q_j] + \int_0^T \mu_j(t) \dot{q}_j(t) dt \geq 0 \quad (46)$$

of the fluid due to the radiation potential ϕ_R is thus supplied to the fluid by interaction with the ship. Energy-flow arguments lead to the conclusion that the time derivative of the energy V_R is equal to the power supplied from the ship motion, i.e.

$$\dot{V}_R = \dot{\mathbf{q}}^T \boldsymbol{\tau}^R = \sum_{k=1}^6 \dot{q}_k \tau_k^T \quad (47)$$

This implies that the mapping $\dot{\mathbf{q}} \mapsto \boldsymbol{\tau}^R$ is passive (Lozano *et al.*, 2000). Passivity is a structural property of the model that can be used to check the validity of model representations (Kristiansen and Egeland, 2003).

4.2. Positive realness

The Laplace transformation of the convolution integral is

$$\mathcal{L} \left\{ \int_{-\infty}^t K_{jk}(t-\sigma) \dot{q}_k(\sigma) d\sigma \right\} = s \tilde{K}_{jk}(s) \tilde{q}_k(s) \quad (48)$$

where $\tilde{K}_{jk}(s) = \mathcal{L}\{K_{jk}(t)\}$, $\tilde{q}_k(s) = \mathcal{L}\{q_k(t)\}$, and where it is used that $\mathcal{L}\{\dot{q}_k(t)\} = s \tilde{q}_k(s)$. The Laplace transformation of the equation of motion (12) is then found to be

$$\sum_{k=1}^6 ((m_{jk} + a_{jk})s^2 + (b_{jk} + \tilde{K}_{jk}(s))s + c_{jk}) \tilde{q}_k(s) = \tilde{\tau}_j^D(s) + \tilde{\tau}_j^A(s) + \tilde{\tau}_j^E(s) \quad (49)$$

Considering Equation (49), and defining $\tilde{\mathbf{K}}(s) = \{K_{ij}(s)\}$ as the Laplace transform of the impulse response function $K_{ij}(t)$, the Laplace transformation of the radiation force by the vessel motion $\dot{\mathbf{q}}$ can be written

$$\tilde{\boldsymbol{\tau}}^R(s) = \left[\mathbf{A}s + \mathbf{B} + \tilde{\mathbf{K}}(s) + \frac{1}{s} \mathbf{C} \right] s \tilde{\mathbf{q}}(s) \quad (50)$$

where

$$\mathbf{A} = \{a_{ij}\}, \quad \mathbf{B} = \{b_{ij}\} \quad (51)$$

$$\tilde{\mathbf{K}}(s) = \{\tilde{K}_{ij}(s)\}, \quad \mathbf{C} = \{c_{ij}\} \quad (52)$$

The passivity of the mapping $\dot{\mathbf{q}} \mapsto \tau_{\mathbf{R}}$ implies that the transfer function matrix

$$\tilde{\mathbf{H}}_{\mathbf{R}}(s) = \mathbf{A}s + \mathbf{B} + \tilde{\mathbf{K}}(s) + \frac{1}{s} \mathbf{C} \quad (53)$$

is positive real. This implies that

$$\tilde{\mathbf{H}}_{\mathbf{R}}(j\omega) + \tilde{\mathbf{H}}_{\mathbf{R}}(j\omega)^* \geq 0, \quad \forall \omega \neq 0 \quad (54)$$

5. Generation of approximate low order state-space model

This section presents a demonstration of the proposed method for the calculation of a low order state-space representation of the radiation force convolution term. Frequency dependent added mass $\alpha_{jk}(\omega)$ and damping $\beta_{jk}(\omega)$ for a ship can be calculated numerically using software packages such as WAMIT, which is a commercially available program package developed by WAMIT Inc. WAMIT is a radiation/diffraction panel program developed for linear analysis of the interaction of surface waves with offshore structures. WAMIT is based on a 3D panel method, utilizing Green's theorem to derive integral equations for the radiation and diffraction velocity potentials on the body boundary. The free surface boundary condition and body boundary condition are linearized, and the flow is assumed to be potential, harmonic and free of separation or lifting effects. Thus, only the case with no mean forward speed is considered here. For further details, see Newman and Lee (2004).

In this work, a 3400 panel hull geometry of an approximately 110 m long, 6000 tonnes deadweight offshore support vessel is used with WAMIT version 6. The hull geometry data is assumed to be symmetric about the xz -plane. Values for $\beta_{jk}(\omega)$ were calculated in the frequency range $0.1 < \omega < 6.5$ rad/s using 0.1 rad/s intervals. Two of the coefficients are shown in Figures 2 and 3. Note the large differences between the maximum and minimum values, in some coupling modes the force even changes sign. Variations in some of the coefficients at high frequency, seen here in the coupling mode between sway and roll, shown in Figure 3, are expected to be related to the panel size in the hull geometry. Moreover, note that the peak at $\omega \approx 3$ rad/s in Figure 3 is expected to be an irregular frequency. Although WAMIT has an option for removing such irregular frequencies, this was not utilized here.

5.1. System identification

The convolution term kernels, or impulse responses, $K_{jk}(t)$ are calculated from (19). $K_{jk}(t)$ is found by trapezoidal integration over ω with $\Delta\omega = 0.01$ for each t , spaced by the time-step $h = 0.05$ s. Any other integration method could have been applied. A splines method has also been tested, but as the results were not significantly better, the trapezoidal integration method was chosen for simplicity. To capture the wanted dynamics, the upper limit for t must be chosen after $K_{jk}(t)$ converges. Here, the upper limit was taken to be 15 s, which is just after $K_{jk}(t)$ converges to zero for all modes.

The state-space model is generated from $K_{jk}(t)$ by applying the system identification scheme based on the Hankel singular value decomposition method proposed by Kung (1978), available as the function IMP2SS in the Robust Control Toolbox of MATLAB. A following scaling of the output matrices \mathbf{C}_{jk} and \mathbf{D}_{jk} with the time-step h , produces the high-order system matrices $\bar{\mathbf{A}}_{jk}$, $\bar{\mathbf{B}}_{jk}$, $\bar{\mathbf{C}}_{jk}$ and $\bar{\mathbf{D}}_{jk}$.

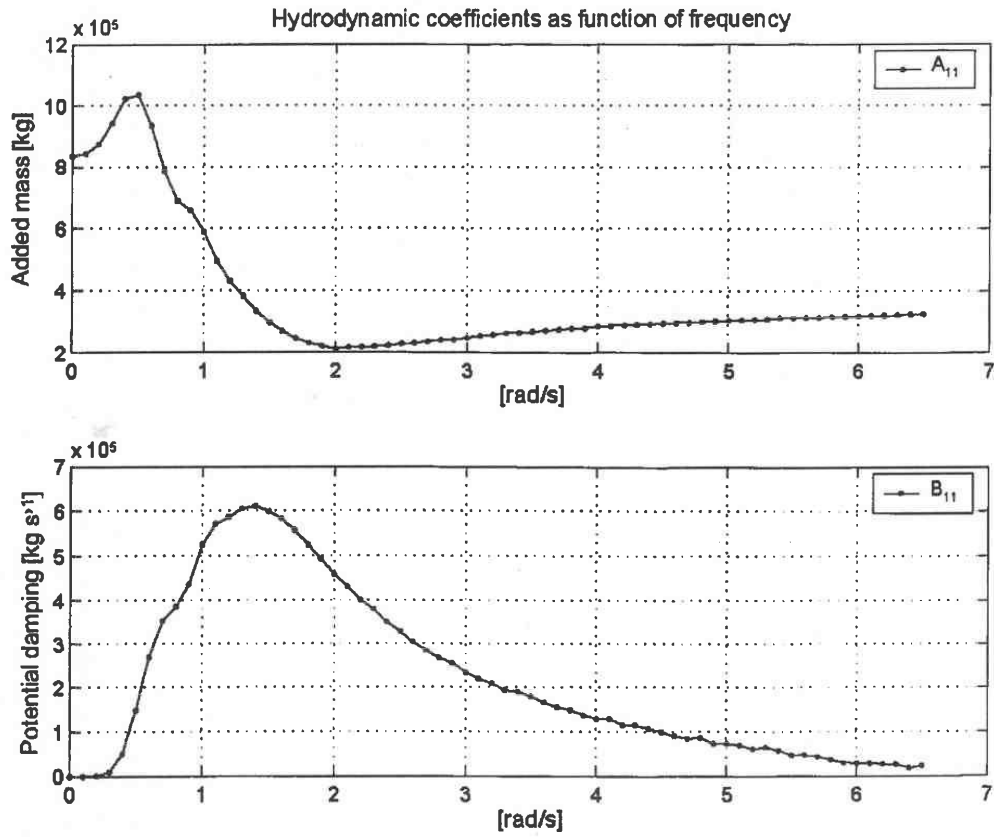


Figure 2. Hydrodynamic coefficients in surge.

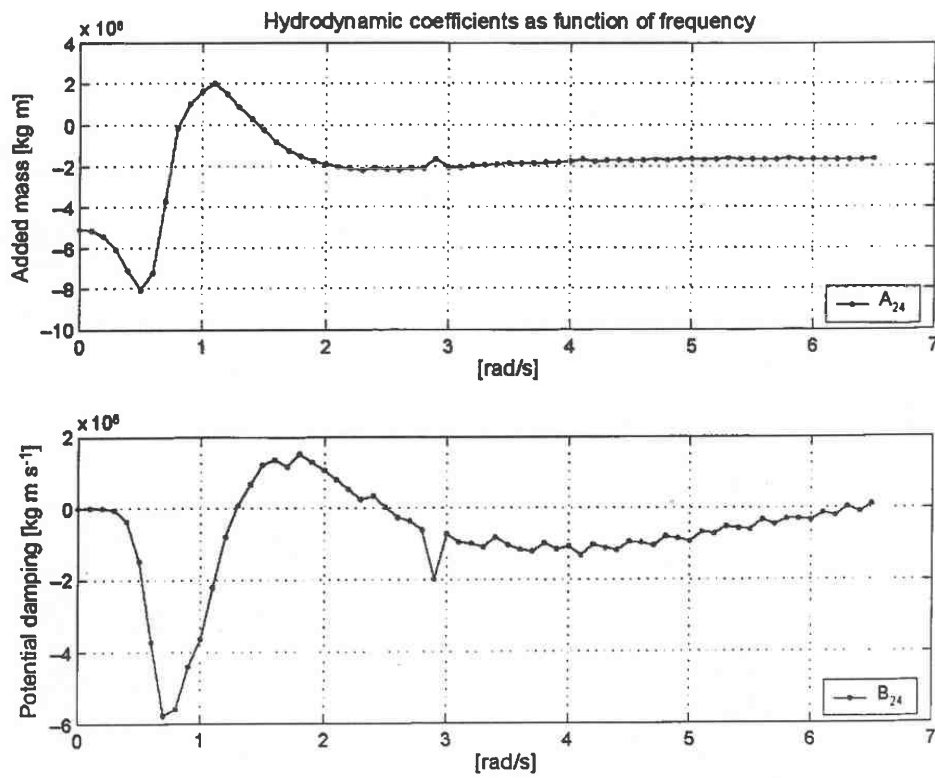


Figure 3. Hydrodynamic coefficients in coupling mode sway-roll.

5.2. Model reduction

The state-space model from IMP2SS is of high order. The order can be controlled indirectly, by giving an explicit bound of the H^∞ -norm of the error between the approximate realization and the exact realization as a parameter in the IMP2SS-function. If no such parameter is given, a default bound is used, yielding a state-space model with high order.

The original model order is proportional with the number of data points given by the ratio T/h , and is close to 280 in several modes. As the model order is directly connected to the number of data points rather than the dynamics of $K_{jk}(t)$, one may expect that significant reduction of the model order of the state-space model can be achieved while retaining the desired properties of the state-space approximation. Such properties can be small approximation error or preservation of stability and passivity.

As a desired property of the method to generate a state-space approximation of the radiation force is to control the accuracy and model order, the truncated balanced reduction method with Lyapunov balancing is selected. Moreover, the original model order is no larger than 280 due to the rate of which $K_{jk}(t)$ converges and the temporal resolution chosen, which is in model order a range where the truncated balanced reduction method will be computationally efficient.

The truncated balanced reduction method is implemented in a numerically robust way in the Matlab function BALMR from the Robust Control Toolbox. See Safonov and Chiang (1989) for details. The output is the new low order state-space matrices \mathbf{A}_{jk} , \mathbf{B}_{jk} , \mathbf{C}_{jk} and \mathbf{D}_{jk} . Models of order between 3 and 12 have been calculated in relation to this work.

5.3. Results

The system equations have now been restated as

$$\sum_{k=1}^6 (m_{jk} + a_{jk}) \ddot{q}_k = - \sum_{k=1}^6 b_{jk} \dot{q}_k - \sum_{k=1}^6 c_{jk} q_k - \sum_{k=1}^6 \mu_{jk} + \tau_j^D + \tau_j^A \quad (55)$$

$$\dot{\xi}_{jk} = \mathbf{A}_{jk} \xi_{jk} + \mathbf{B}_{jk} \dot{q}_k \quad (56)$$

$$\mu_{jk} = \mathbf{C}_{jk} \xi_{jk} + \mathbf{D}_{jk} \dot{q}_k \quad (57)$$

Note that here τ_j^E is omitted, as no external forces exist in this work. The results of the model identification and reduction, and thereby the verification of the accuracy of the reduced model, can be visualised by plotting the impulse responses of the approximated low order state-space models together with the original impulse response functions $K_{jk}(t)$. This is shown in Figures 4 and 5 for two modes. Here i in μ_{jk}^i denotes the order of the approximated state-space system. Note that the impulse response function for $K_{24}(t)$ shown in Figure 5 has small oscillations for t near the upper limit of $t = 15$ s. The period of this oscillation is approximately $T \approx 2$ s, which is consistent with the irregular frequency of $\omega \approx 3$ rad/s seen in Figure 3.

Another property used to check the validity of the low order state-space model is the structural property of passivity. As Lyapunov balancing was selected in the model reduction, there is no guarantee of retaining any passivity properties. However, this can easily be examined by checking the Nyquist plots for positive realness. In Figures 6 and 7, the Nyquist plot for the diagonal element μ_{22}^i and μ_{44}^i for $i = 3-5$ are plotted. In this work, $\tilde{K}_{44}^4(s)$ and $\tilde{K}_{44}^5(s)$ are positive real, while $\tilde{K}_{44}^3(s)$ is not positive real. But in sway,

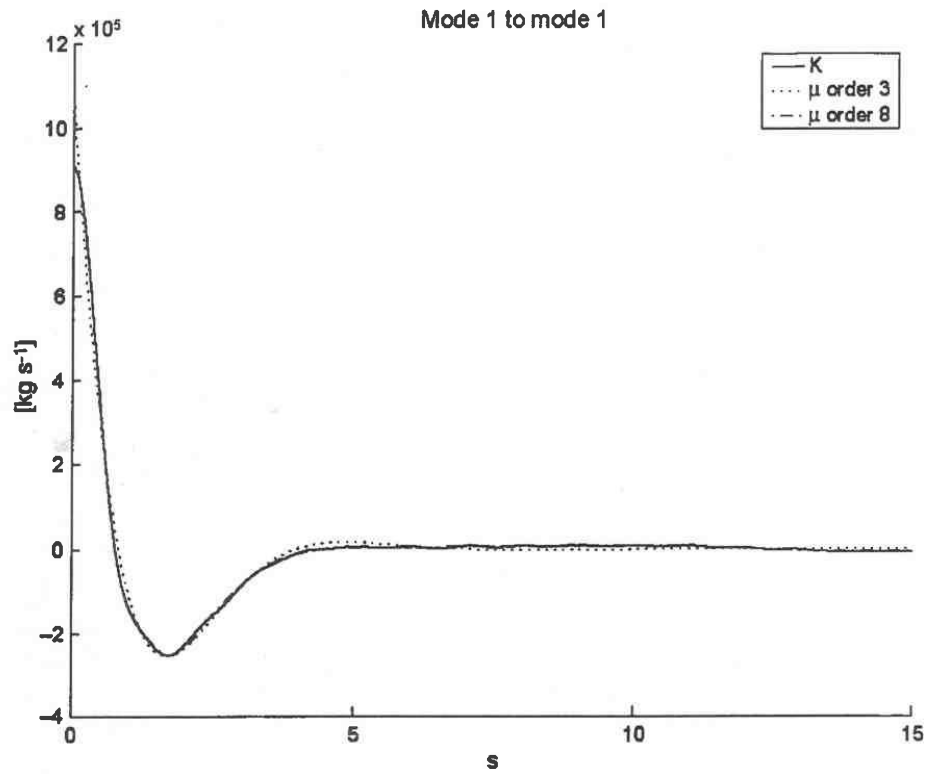


Figure 4. Impulse response in surge.

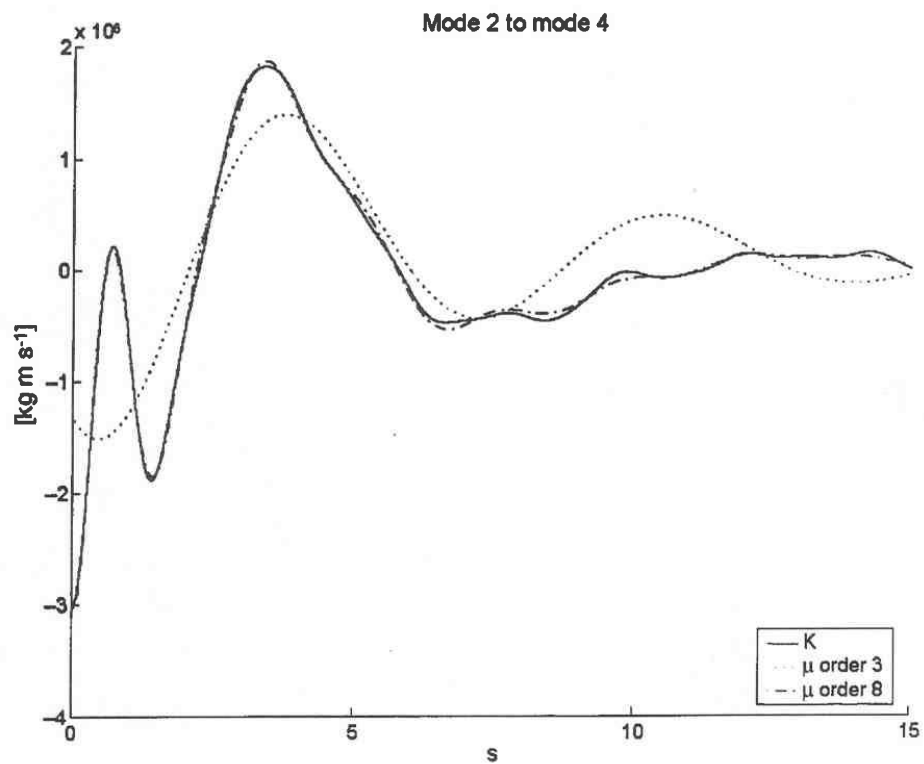


Figure 5. Impulse response in coupling mode sway-roll.

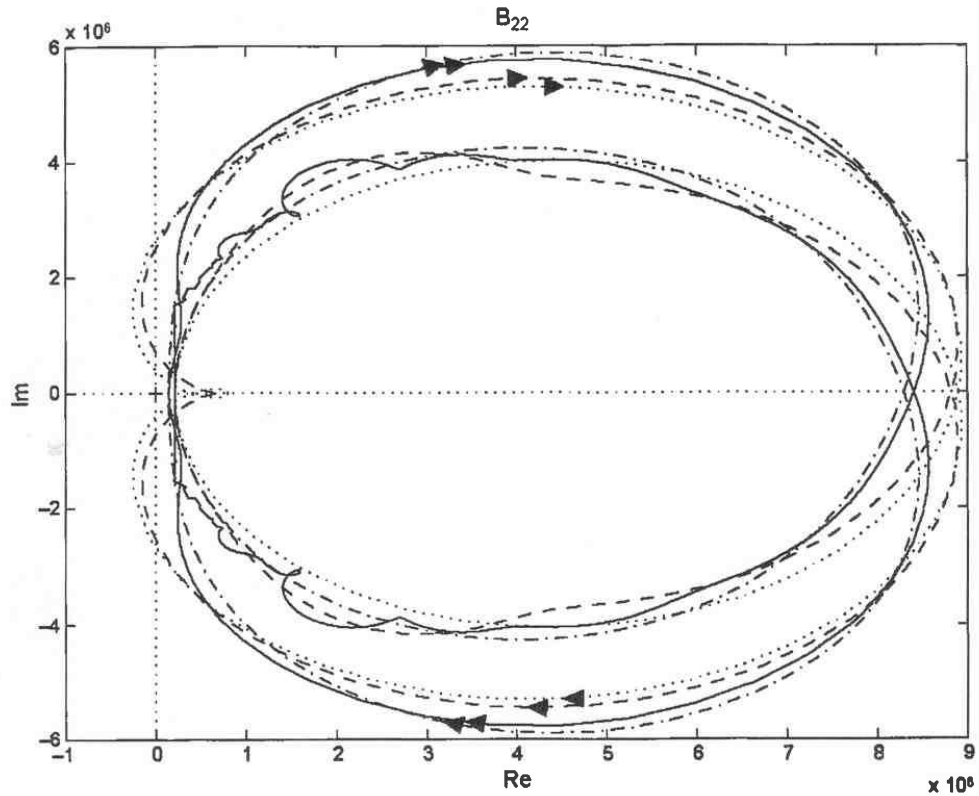


Figure 6. Nyquist diagram of $\tilde{K}_{22}^i(s)$, where i denotes the approximation order, $i = 5$ (dashed), $i = 4$ (dash-dotted) and $i = 3$ (dotted), impulse response function before reduction (solid).

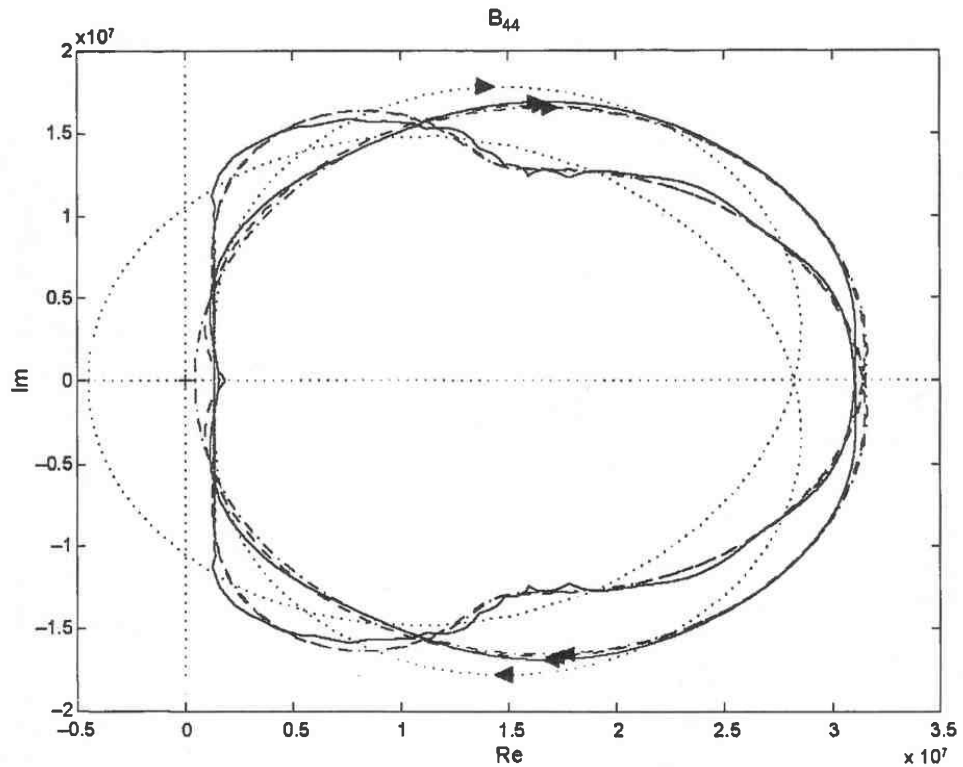


Figure 7. Nyquist diagram of $\tilde{K}_{44}^i(s)$, where i denotes the approximation order, $i = 5$ (dashed), $i = 4$ (dash-dotted) and $i = 3$ (dotted), impulse response function before reduction (solid).

even $\tilde{K}_{22}^S(s)$ is not positive real. Note that different modes have different lower boundaries of the available order of the state-space models to ensure valid energy properties of the approximated system. In the simulations that follow, eighth-order state-space models are used.

6. Simulations

6.1. Setup

The equations of motion used in the simulations are

$$\sum_{k=1}^6 (m_{jk} + a_{jk}) \ddot{q}_k = - \sum_{k=1}^6 b_{jk} \dot{q}_k - \sum_{k=1}^6 c_{jk} q_k - \sum_{k=1}^6 \mu_{jk} + \tau_j^D + \tau_j^A \quad (58)$$

$$\dot{\xi}_{jk} = \mathbf{A}_{jk} \xi_{jk} + \mathbf{B}_{jk} \dot{q}_k \quad (59)$$

$$\mu_{jk} = \mathbf{C}_{jk} \xi_{jk} + \mathbf{D}_{jk} \dot{q}_k \quad (60)$$

where the radiation force is found utilizing the method presented in Section 3.

The vessel is simulated in six degrees of freedom excited with long-crested waves. Thus, the sea state is described using a JONSWAP spectrum with 8 s peak wave period and 2 m significant wave height. Wave elevation and wave loads are calculated using superposition of 1000 wave components, with wave load $\tau_j^D(t)$ in mode j given by

$$\tau_j^D(t) = \sum_i K_{j,i}^D A_i \sin(\omega_i t - k_i x \cos \theta_i - k_i y \sin \theta_i + \phi_{j,i} + \epsilon_i) \quad (61)$$

where A_i is the amplitude of component i at frequency ω_i

$$A_i = \sqrt{2S(\omega_i)\Delta\omega} \quad (62)$$

k_i is wave number ($k_i = \omega_i^2/g$), x and y are vessel position, $K_{k,i}^D$ and $\phi_{j,i}$ represent force response amplitude and phase, and ϵ_i is a random phase for each wave component. $K_{j,i}^D$ and $\phi_{j,i}$ vary with the wave frequencies and the direction of the incoming waves relative to the vessel heading, and are calculated by WAMIT.

Simple control forces τ_j^A are added to keep the vessel near equilibrium. Position is controlled using a simple limited PD-controller and a fully actuated thruster configuration in the horizontal plane yielding a corrective force

$$\tau_j^A(s) = P_{jk} \frac{1 + T_d s}{1 + \alpha T_d s} (\bar{q}_{ref,j}(s) - \bar{q}_j(s)) \quad (63)$$

where $P_{jk} = m_{jk}/40$, $T_d = 15$ s and $\alpha = 0.01$. In order to avoid exciting the vessel with a step from suddenly activating wave loads at $t = 0$, the wave loads increase, during the first 30 s of the simulation.

All coefficients are calculated from WAMIT using the same frequency interval as the hydrodynamic coefficients. Further, all coefficients are calculated for nine evenly spaced wave headings between 0 and 180°. Values for all headings are calculated using symmetry and linear interpolation.

The kinematics are modelled as a rigid body influenced by forces in the body frame. Although linear theory assumes forces apply on the mean hull position in the equilibrium frame, the small motion assumption justifies this approach. The kinematics block is general, using the total inertia matrix (6×6 rigid body inertia and added mass) as a

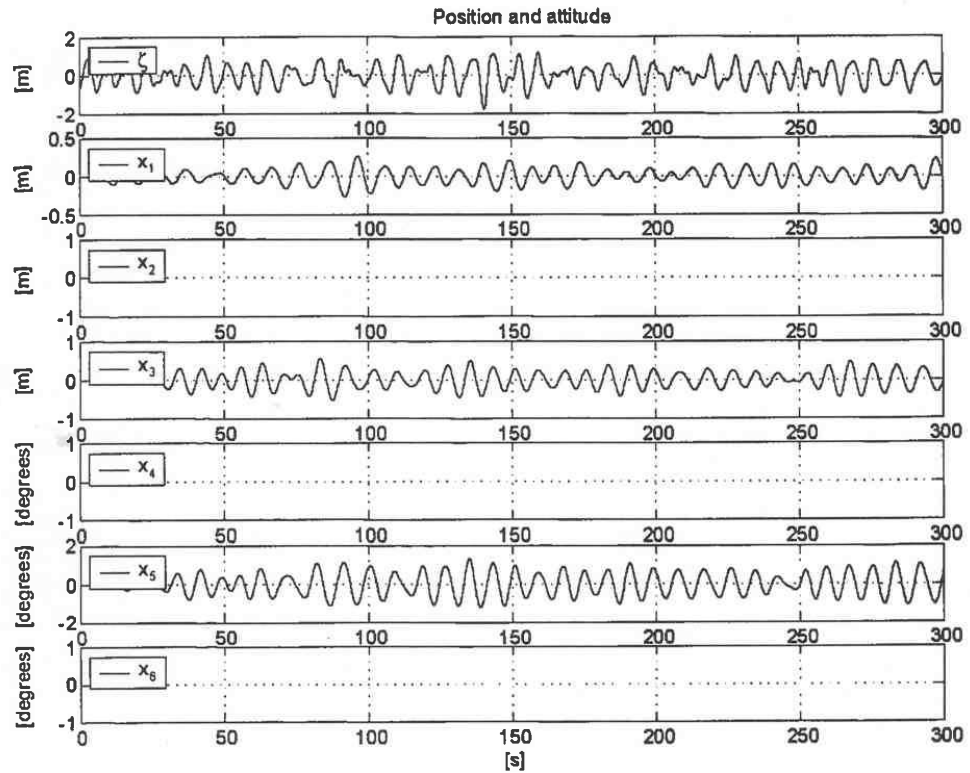


Figure 8. Motion in head sea.

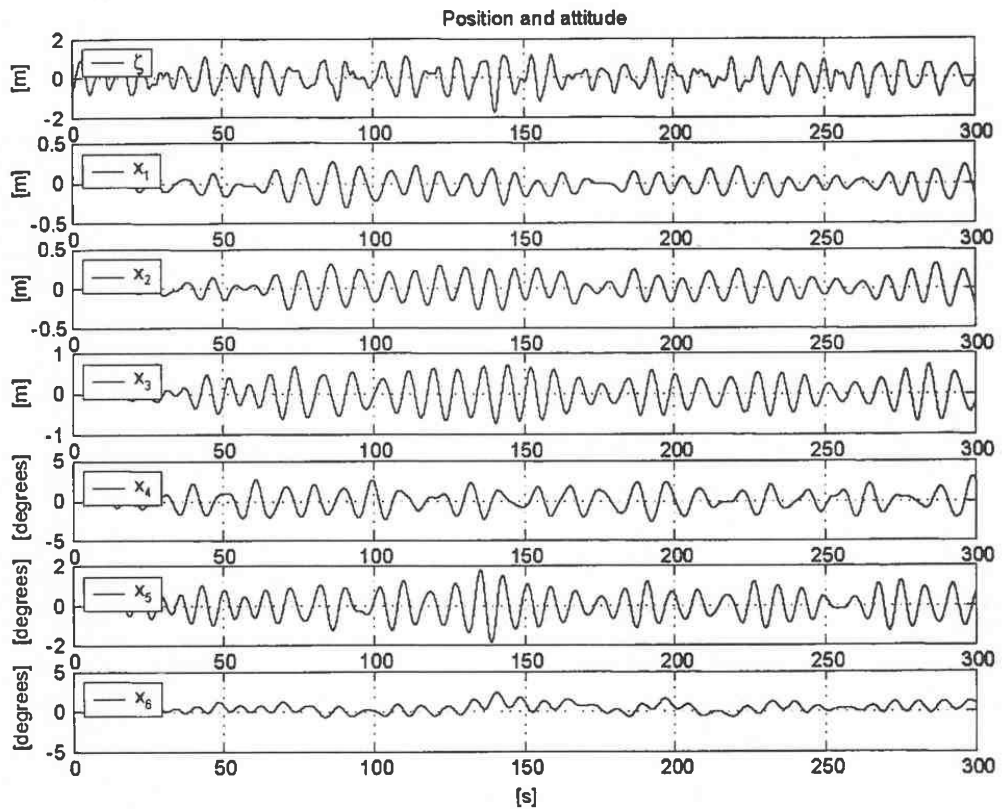


Figure 9. Motion in quartering sea from starboard.

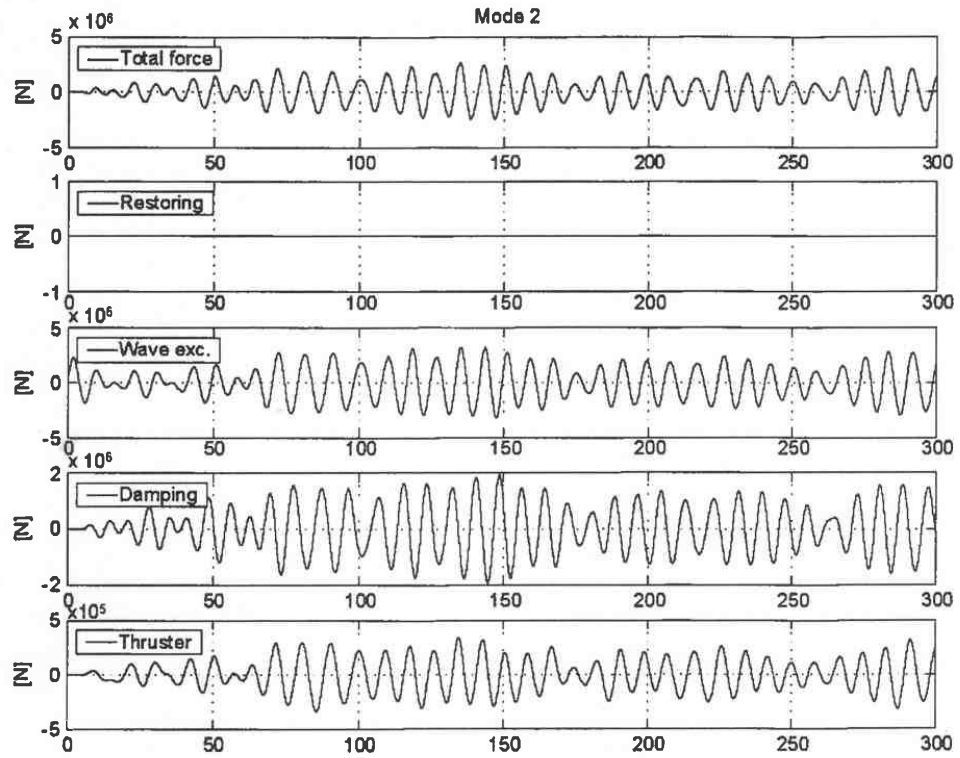


Figure 10. Forces in sway, quartering sea.

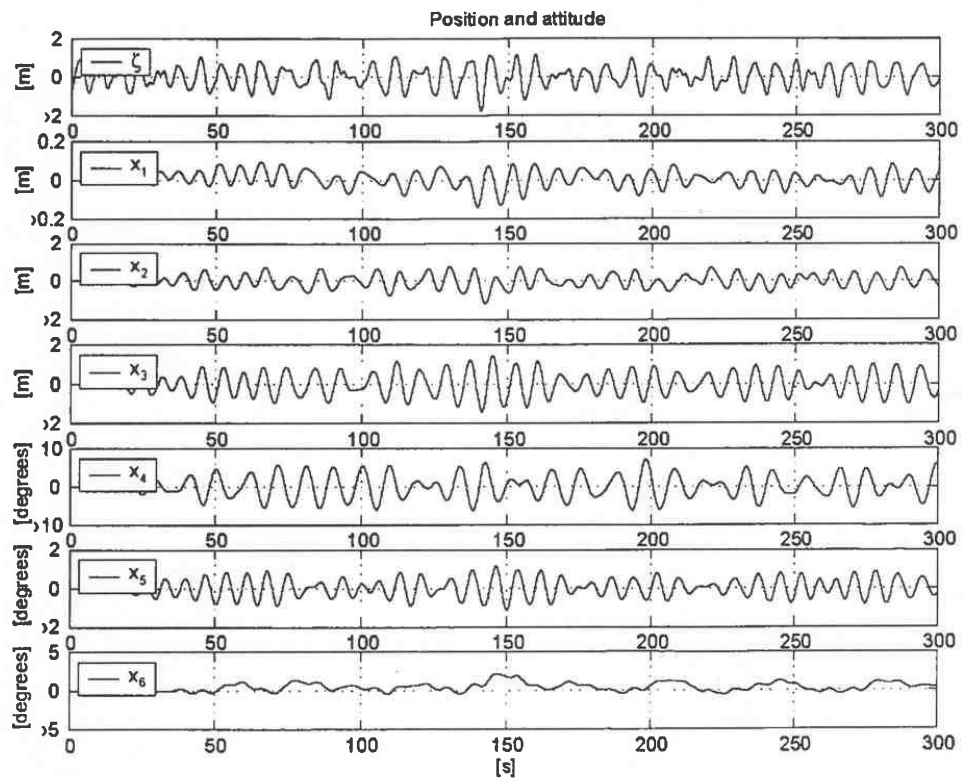


Figure 11. Motion in sea from starboard.

single parameter. The separate force contributions; radiation, diffraction and restoring forces are calculated in separate blocks. The dynamics are modelled as linear, and superposition is assumed.

The simulations are done using Matlab/Simulink on a 2.4 GHz Pentium IV. Using eighth-order approximations of the radiation force (for each coupling mode, for a total of 144 states) and recalculating the wave exciting force from 1000 wave components every 0.3 s, 300 s of simulation time took little more than 20 s.

6.2. Results

Figure 8 shows the responses in all modes for head sea. The significant wave amplitude was 1 m. In heave, the response amplitude operator (RAO) was 0.3 at the peak frequency and this is in agreement with the observed heave response with amplitude about 0.3 m. In pitch, the RAO was 1.03 at the peak frequency and this is in agreement with the observed pitch motion with amplitude about 1 m. This simple test indicates that the wave motion calculated from the WAMIT model is of the right order of magnitude.

Figure 9 shows the ship motion with waves coming from 45° starboard of the ships heading (quartering sea). The waves now excite all modes. The response in heave is now larger than in Figure 8, as should be expected. The various force contributions in sway for the motions shown in Figures 9 and 10.

In Figure 11, the waves approach from starboard. Comparing with quartering sea, motion in sway increases. There is still surge motion, caused by coupling effects from heave and pitch.

7. Conclusions

The forces from the radiation potential and the resulting equation of motion for harmonic motions are commonly described using hydrodynamic coefficients that are frequency-dependent. This results in a model formulation that only is valid for harmonic motion, and which does not convert easily to the standard formulations used in automatic control. The frequency dependence can be explained by including a convolution term in the expression for the forces from the radiation potential, or more correctly, the model representation utilizing a convolution term can be simplified into a frequency-dependent model formulation. This paper has described the successful application of model identification and reduction techniques using these convolution terms as input, resulting in low order state-space models of the radiation forces. Further, this paper outlines a procedure for generating a low order state-space model that can be utilized with other physical systems represented by convolution terms.

To ensure retaining energy properties of the system, the necessary model order varies between the different modes and couplings. In surge, a third-order model appears sufficient, whereas in the coupling mode between sway and roll with the most complex dynamics an eighth-order model seems necessary.

Comparing the approximate state-space model order with the number of data points in $K_{jk}(t)$, the calculation of the radiation forces for simulation purposes is more efficient using an approximate state-space model than evaluating the convolution integral directly.

References

- ANTOULAS, A. & SORENSEN, D. (2001). Approximation of large-scale dynamical systems: an overview, Presented at MTNS, Perpignan, June 19–23, 2000.

- CUMMINS, W. (1962). The impulse response function and ship motions. *Schiffstechnik*, 101–109.
- EGELAND, O. & GRAVDAHL, J. (2002). Modeling and simulation for automatic control. *Marine Cybernetics*.
- FOSSEN, T. (1994). *Guidance and Control of Ocean Vehicles*. Wiley, New York.
- GUGERCIN, S. & ANTOULAS, A. (2000). A comparative study of 7 algorithms for model reduction, *Proceedings of the 39th IEEE Conference on Decision and Control 2000*; pp. 2367–2372.
- KRISTIANSEN, E. & EGELAND, O. (2003). Frequency-dependent added mass in models for controller design for wave motion damping, *Sixth IFAC Conference on Manoeuvring and Control of Marine Craft 2003*; pp. 90–95.
- KUNG, S. (1978). A new identification and model reduction algorithm via singular value decompositions, *Proceedings of 12th Asimolar Conference on Circuits, Systems and Computers 1978*; pp. 705–714.
- LOZANO, R., BROGLIATO, B., EGELAND, O. & MASCHKE, B.I. (2000). *Dissipative Systems Analysis and Control*. Springer, London.
- NEWMAN, J. (1977). *Marine Hydrodynamics*. MIT Press, Cambridge, MA.
- NEWMAN, J. & LEE, C. H. (2004). *WAMIT User Manual*, WAMIT Inc. <http://www.wamit.com/manual.htm>.
- OGILVIE, T. (1964). Recent progress toward the understanding and prediction of ship motions, *The Fifth Symposium on Naval Hydrodynamics 1964*; pp. 3–128.
- SAFONOV, M. & CHIANG, R. (1989). A Schur method for balanced model reduction. *IEEE Transactions on Automatic Control* AC-34 (7), 729–733.
- YU, Z. & FALNES, J. (1998). State-space modelling of dynamic systems in ocean engineering. *Journal of Hydrodynamics*, 1–17.
- YU, Z. & FALNES, J. (1995). State-space modelling of a vertical cylinder in heave. *Applied Ocean Research* 17 (5), 265–275.